AMSE JOURNALS-AMSE IIETA publication-2017-Series: Modelling C; Vol. 78; N°1; pp 116-124
Submitted Jan. 2017; Revised March 15, 2017, Accepted April 15, 2017

Thermal Behavior and Phase Formation of the Strontium Cobalt Oxides Prepared via Sol-Gel Method

Sofiane Makhloufi.[*], Mahmoud Omari.[**]

[*,**] Laboratory of Molecular Chemistry and Environment, University of Biskra, B. P. 145, 07000 Biskra, Algeria (makhloufi_sofiane@yahoo.fr)

Abstract

Our contribution has focused on the synthesis and characterization of strontium cobalt SrCoO3-δ oxide by the Sol-Gel method. The powder was successfully synthesized using citric acid, Sr (NO3)2 and Co (NO3)2.6H2O as raw materials by this method and calcined at different temperatures. It was characterized by several techniques: Fourier transform infrared spectroscopy (FT-IR), thermogravimetric and differential thermal analysis (TGA/DTA), X-ray diffraction (XRD) and laser diffusion. All the results for physico-chemicals characterizations show that the crystallization temperature of the SrCoO3-δ precursor gels is estimated as 900 °C by TG/DTA. The XRD pattern of the SrCoO3-δ precursor gels calcined at 950 °C for 6 h has a perovskite structure of rhombohedral phase formed and the presence of crystalline impurities is not found. The crystallite size of SrCoO3-δ slightly increases from 23,02 to 38,13 nm with calcination temperature increasing from 750 to1050 °C for 6 h.

Keywords

Perovskite, Rhombohedral $SrCoO_{3-\delta}$, Sol-Gel method, Strontium cobalt oxides, Thermal analysis.

1. Introduction

Perovskite-type oxides have attracted great interest in both applied and fundamental areas of solid state chemistry, physics, advanced materials, and catalysis [1]. The family of compounds with ABO_3 structure containing strontium and cobalt in their A and B sites respectively has received a great attention due to their high electronic conductivity and oxygen ionic conductivity. [2, 3].

$SrCoO_{3-\delta}$ composite is an important parent compound for the development of a series of functional materials. Depending on the operating temperature, oxygen partial pressure of the environment, thermal history, and synthesis method, strontium cobaltite present 2-H type hexagonal perovskite, oxygen vacancy-ordered brownmillerite, rhombohedral perovskite, or cubic perovskite structure [4, 5]. Another study has revealed that the phase structure and electrical conductivity of $SrCoO_{3-\delta}$ oxide were closely related with the oxygen content in the composite. [6].

These complex oxides can be properly modified by the partial substitution of atoms at A and / or B sites which may affect strongly their physical properties. Indeed, depending on the doping component and level, the material can display ferromagnetic or thermo-electrical properties [7] and electrochemical properties [2, 3]. $SrCoO_{3-\delta}$ doped with various metal ions such as Nb [8], Sc [9], Sb [3], Ca and Fe [5], Ce and Fe [2, 10], were previously studied. These oxides have been identified as promising IT-SOFC cathode materials and oxygen transport membranes.

A few years ago, several studies have shown that nickel catalysts were active for reforming of methane [11, 12]. On the other hand, another work on Ni-doped perovskite anodes for oxidation of hydrogen in IT-SOFC has been carried out [13]. It has been revealed that suitable power densities of about 420 mW/cm^2 for the direct oxidation of hydrogen were achieved at 800 °C.

Despite these advantages, there have been no reports to date concerning the synthesis and characterization of strontium cobaltite oxides. In the present work, we examine the Thermal behavior, grain morphology, electrical conductivity and electrochemical properties of $SrCoO_{3-\delta}$ oxides prepared by the sol–gel method.

2. Experimental Procedure

2.1 Synthesis

$SrCoO_{3-\delta}$ oxide was prepared by a sol-gel method using citric acid as a complexing agent. Aqueous solutions of $Sr(NO_3)_2$ (BIOCHEM), $Co(NO_3)_2.6H_2O$ (BIOCHEM 98.5%) were first dissolved in absolute formaldehyde (methanal) separately. The molar amount of citric acid was equal to total molar amount of metal nitrates in solution. Citric acid (Biochem) was added to the precursors under vigorous stirring. The homogeneous solution obtained was heated at 80-90 °C for 4 h.To remove the solvent, the gel is heated for 24 h at 100 °C. The resulting precursor is then milled and calcined in air for 6 h at different calcination temperatures: 650, 750, 850, 950 and 1050 °C with a heating rate of 5 °C min^{-1}.

2.2 Characterization Techniques

The thermal decomposition processes of the precursor gels were studied in air atmosphere by TGA Schimadzu with a heating rate of 10 °C/min, from room temperature to 1000°C.

Infrared transmission spectra were performed on a Fourier transform spectrometer (FTIR) Shimadzu 8400S. A granular technique employing KBr (1 mg of sample added to 200 mg of KBr) was used, and the spectra were recorded in the 400–1300 cm^{-1} range.

X rays diffraction (XRD) patterns were collected on a Bruker AXS D8 advance diffractometer employing Cu Ka radiation. In all diffractograms, a step size of 0.02° (2Θ) was used with a data collection time of 15 s. Data were collected between 2Θ values from 10° to 80° using standard Θ/2Θ geometry. Identification of crystalline phases was carried out by comparison with JCPDS standards. The unit cell parameters were obtained by fitting the peak position of the XRD pattern using the CELREF and X'pert Highscore programs. Moreover, morphological aspects of the powders were examined by using an ESEM-FEI Quanta 600 FEG scanning electron microscope (SEM).

3. Results and Discussion

3.1 Thermogravimetric Analysis

The mechanism of the thermal decomposition in flowing air of $SrCoO_{3-\delta}$ precursor gel was studied by TG/DTA measurements. The TG/DTA profiles for this sample are shown in Figure 1. In TG curve, there are four regions of weight loss: (1) 25-100 °C, (2) 100-200 °C, (3) 200-540 °C, and (4) 820-920 °C with corresponding organic weight losses of 5%, 8%, 40% and 8%, respectively. At the first region of weight loss, water and gases adsorbed on the powder surface were eliminated, with an endothermic transition at 80 °C. The second region of mass loss, can be ascribed to the removal of the residual water and a partial decomposition of citric acid chain, accompanied a broad exothermal peak around 180°C in DTA curve. The third step was assigned to the combustion of the organic material between 200 and 540 °C (mass loss -40%), with a strong and large exothermic peak in the DTA curve, which contains two endothermic peaks. These peaks probably correspond to the formation of the strontium carbonate [14]. The last small endothermic peak was observed at about 870 °C, can be attributed to the formation of the $SrCoO_{3-\delta}$ crystal, as was confirmed by XRD results, discussed below.

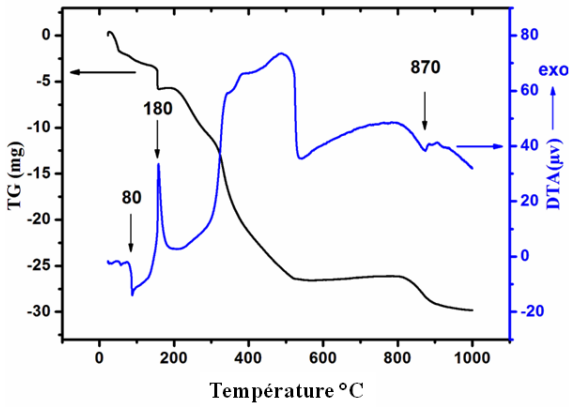

Fig.1. Thermogravimetric profiles of $SrCoO_{3-\delta}$ precursor

3.2 X-ray Diffraction

XRD experiments were first performed to check the phase purity of the materials. Figure 2 shows the XRD patterns of $SrCoO_{3-\delta}$ calcined at different temperatures for 6 h. After calcination at 650 °C, the precursor is a mixture containing orthorhombic $SrCO_3$ (PDF: 01-074-1491) and spinel Co_3O_4 (PDF: 01-076-1802). When the precursor was heated at 750 °C in air for 6 h, the characteristic diffraction peaks of Co_3O_4 and $SrCO_3$ become weaker while those of rhombohedral structure appear. With the increase of calcination temperature, the intensity of characteristic diffraction peaks of Co_3O_4 and $SrCO_3$ becomes weaker at 850 °C and disappears at 950 °C. The intensity of characteristic diffraction peaks of rhombohedral structure becomes stronger and no reflections from strontium oxide and cobalt oxide are observed as distinct intermediate phases to the formation of $SrCoO_{3-\delta}$ during the thermal decomposition of the precursor powder. After heat treatment at 950 °C, the precursor shows good crystallinity of the rhombohedral structure of $SrCoO_{3-\delta}$. These XRD patterns confirm that the sample maintain the rhombohedral perovskite structure (PDF card 00-049-0692) at temperatures higher than 650 °C.

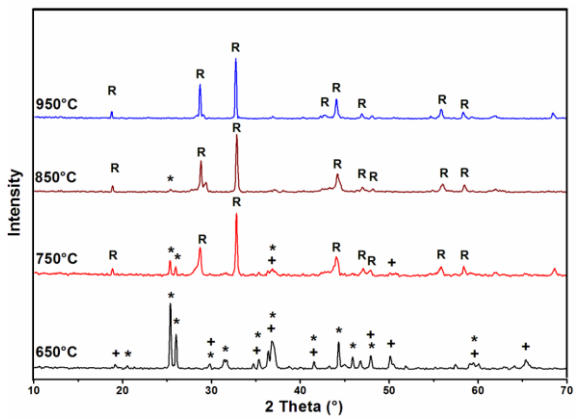

Fig.2. XRD patterns of the $SrCoO_{3-\delta}$, at different temperatures.

3.3 IR Spectroscopy

The vibration frequencies in the infrared region are fundamental for the control of the reaction process and properties of materials. Fourier transformed infrared spectroscopy results of $SrCoO_{3-\delta}$ precursor calcined at different temperatures are shown in Figure 3. Five bands were observed at 860, 704, 670, 580 and 480 cm^{-1}. At 650°C, the IR spectra show two strong absorption bands at 670 and 580 cm^{-1}, which confirms the formation of the spinel structure of Co_3O_4 [15, 16]. The first peak is attributed to the stretching vibration mode of M–O in which M is Co^{2+} and is tetrahedrally coordinated [17]. The second peak can be assigned to M–O in which M is Co^{3+} and is octahedrally coordinated [17, 18]. The bands at 860 cm^{-1}, 704 cm^{-1} corresponding to the respective v2 and v4 modes of carbonate [19], mark the existence of $SrCO_3$ [20]. At temperatures higher than 750 °C, the content of $SrCO_3$ decreases and another band at 480 cm^{-1} appears which is characteristic of the rhombohedral perovskite structure. This result further confirms that $SrCO_3$ keep on joining into Co_3O_4 structure and form the perovskite oxide. A similar result was found in Ba $(Fe,Co)O_{3-\delta}$ [21]. It has been shown that $BaCO_3$ will keep on joining into CoO_6 and form the compound $BaCoO_{2.93}$ .These results are in accordance with the XRD analysis (Figure 2). The bands at 860, 704, and 670 cm^{-1} disappear when the precursor was calcined at 950 °C in air which indicates that the decomposition of carbonate has finished. The bands at 580 cm^{-1} and 480 cm^{-1} due to the asymmetric stretching vibrations of Sr-O and Co-O groups [22]. This is in accordance with the XRD results (Figure 2) which confirms the formation of a single crystalline phase in $SrCoO_{3-\delta}$ nanopowder.

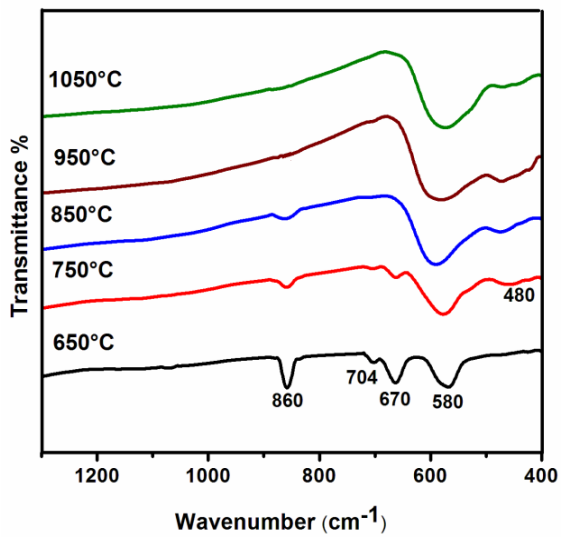

Fig.3. Infrared spectra of $SrCoO_{3-\delta}$ calcined at different temperatures

3.4 Structural and Morphological Characterization

The peak broadening at lower angle is more meaningful for the calculation of particle size, therefore size of nanocrystals. The crystallite size (D) of the samples was calculated from the full width at half maximum of the most intense diffraction peak using Scherrer's equation (Eq. 1): [23].

$$D=\frac{0.8\lambda}{\beta\cos\theta} \quad (1)$$

Where D is the mean crystallite size, ß is the full width at half maximum and λ is the used radiation wavelength (1.54059 Å) and θ is Bragg's diffraction angle.

Figure. 4 show the variation of average crystallite size (DXRD) of the $SrCoO_{3-\delta}$ powders calcined at different temperatures for 6 h. The crystallite sizes calculated from the Scherrer formula are slightly increase in the range of 23.02–38.13 nm respectively with the calcination temperature increasing from 750 to 1050°C. This distinction can be caused of synthesis parameters such as chemical nature of the base solvant that affects on the morphological characteristics of the nanoparticles $SrCoO_{3-\delta}$ powders.

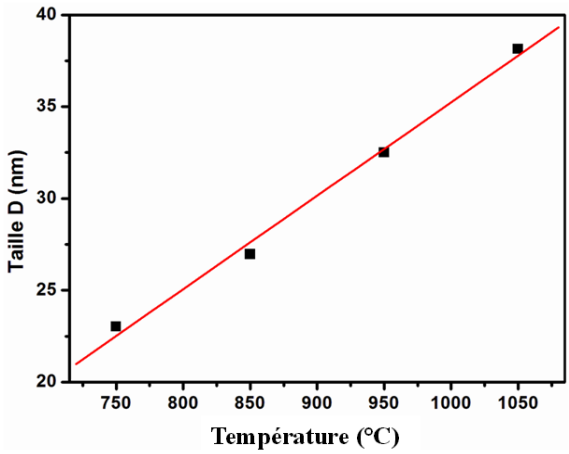

Fig.4. Crystallite size of $SrCoO_{3-\delta}$ powders calcined at different temperatures for 6 h

The SEM micrographs of the SrCoO3-δ compounds are shown in Fig 5. A different surface morphology for all samples is observed. Particles are large and have an inhomogeneous dispersion of particle sizes. The powder is constituted by the aggregation of various dimensions and forms of particles with the grain size greater than 1µm. The formation of agglomerate is probably due to the nature of the solvent used in the preparation of the precipitate. The same result was also found for samarium-doped ceria powders [24]. It has been shown that treating the precipitate with water and ethanol allows interactions between particles which lead during drying to the formation of chemical bonds.

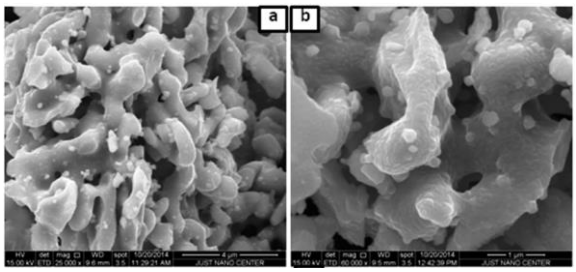

Fig.5. SEM micrographs of $SrCoO_{3-\delta}$

Conclusions

Nanocrystalline Strontium Cobaltat powders have been successfully synthesized at low temperature by Sol-Gel Method using citric acid as a complexing agent, Strontium and cobalt nitrate solutions. When the $SrCoO_{3-\delta}$ precursor powders are formed and calcined at 950°C for 6 h, the pure perovskite $SrCoO_{3-\delta}$ is obtained. No reflection peaks of $SrCO_3$ and Co_3O_4 are observed. The calcination temperature of 950 °C is so far the lowest process temperature for complete $SrCoO_{3-\delta}$ formation. The nanocrystallite size slightly increase from 23.02 to 38.13 nm with the calcination temperature increasing from 750 to 1050 °C, for the SrCoO3-δ precursor powders calcined for 6 h.

References

1. J. Tejuca et al., Properties and Applications of Perovskite-Type-Oxides, 1993, Marcel Dekker.
2. M.T. Colomer, B.C.H. Steele, J.A. Kilner, Structural and electrochemical properties of the $Sr_{0.8}Ce_{0.1}Fe_{0.7}Co_{0.3}O_{3-\delta}$ perovskite as cathode material for ITSOFCs, 2002, Solid State Ionics, vol. 147, pp. 41-48.
3. A. Aguadero, D. Pérez-Coll, C. de la Calle, J.A. Alonso, M.J. Escudero, L. Daza, $SrCo_{1-x}Sb_xO_{3-\delta}$ perovskite oxides as cathode materials in solid oxide fuel cells, 2009, J. Power Sources, vol. 192, pp. 132-137.
4. N. Trofimenko, E.J. Paulsen, H. Ullmann, R. Müller, Structure, Oxygen Stoichiometry and electrical coonductivity in the system Sr-Ce-Fe-O, 1997, Solid State Ionics vol. 100, pp. 201-214.
5. Z.Q. Deng, W.S. Yang, W. Liu, C.S. Chen, Relationship between transport properties and phase transformations in mixed-conducting oxides, 2006, J. Solid State Chem, vol. 179, no. 2, pp. 362-369.

6. V.V. Vashook, M.V. Zinkevich, H. Ullmann, J. Paulsen, N. Trofimenko, K. Teske, Oxygen non-stoichiometry and electrical conductivity of the binary strontium cobalt oxide $SrCoO_x$, 1997, Solid State Ionics, vol. 99, pp. 23-32.
7. A. Maignan, C. Martin, N. Nguyen, B. Raveau, Magnetoresistance in the ferromagnetic metallic perovskite $SrFe_{1-x}Co_xO_3$, 2001, Solid State Sci vol. 3, pp. 57-63.
8. F. Wang, Q. Zhou, T. He, G. Li, H. Ding, Novel $SrCo_{1-y}Nb_yO_{3-\delta}$ cathodes for intermediate-temperature solid oxide fuel cells, 2010, J. Power Sources, vol. 195, pp. 3772-3778.
9. P. Zeng, R. Ran, Z. Chen, W. Zhou, H. Gu, Z. Shao, S. Liu, Efficient stabilization of cubic perovskite $SrCoO_{3-\delta}$ by B-site low concentration scandium doping combined with sol–gel synthesis, 2008, J. Alloys Compd, vol. 455, pp. 465-470.
10. M.D. Carvalho, L.P. Ferreira, M.T. Colomer, P. Gaczynski, M.M. Cruz, J.C. Waerenborgh, M. Godinho, Magnetic studies on $Sr_{0.8}Ce_{0.1}Fe_{0.7}Co_{0.3}O_{3-\delta}$ perovskite, 2006, Solid State Sci. vol. 8, pp. 444-449.
11. Z. Hua Tan, X. Guo, Synthesis and characterization of highly dispersed YSZ particles with diameter ≤ 5nm, 2015, Ceram. Int, vol. 41, pp. 4953-4962.
12. Y. Liu, G. Zhu, B. Ge, H. Zhou, A. Yuan, X. Shen, Concave Co_3O_4 octahedral mesocrystal: polymer-mediated synthesis and sensing properties, 2012, Cryst. Eng. Comm. Vol. 14, pp. 6264-6275.
13. Z. Wen, L. Zhu, Y.G. Li, Z. Zhang, Z.Z. Ye, Mesoporous Co_3O_4 nanoneedle arrays for high-performance gas sensor, Sensors and Actuators, 2014, vol. B 203, pp. 873-879.
14. M. Tatzber, M. Stemmer, H. Spiegel, C. Katzlberger, G. Haberhauer, M.H. Gerzabek, Environ, An alternative method to measure carbonate in soils by FT-IR spectroscopy, 2007, Chem. Lett. vol. 5, pp. 9-12.
15. M.Y. Nassar, I.S. Ahmed, Hydrothermal synthesis of cobalt carbonates using different counter ions: An efficient precursor to nano sized cobalt oxide (Co_3O_4), 2011, Polyhedron, vol. 30, pp. 2431-2437.
16. B. Sreedhar, M. Sulochana, C.S. Vani, D.K. Devi, N.V.S. Naidu, Shape evolution of strontium carbonate architectures using natural gums as crystal growth modifiers, 2014, Eur. Chem. Bull, vol. 3, no. 3, pp. 234-239.
17. P. Ptáčekn, E. Bartoníčková, J. Švec, T. Opravil, F. Šoukal, F. Frajkorová, The kinetics and mechanism of thermal decomposition of $SrCO_3$ polymorphs, 2015, Ceram. Int, vol. 41, pp. 115-123.

18. M. Sun, Y. Jiang, F.F. Li, M.S. Xia, B. Xue, D.R. Liu, Effect of oxygen vacancy variation on the photo-assisted degradation and structural phase transition of oxygen defective Ba(Fe,Co)O_{3-x}, 2011, Mater. Res. Bull, vol. 46, pp. 801-809.
19. A. Leleckaite, A. Kareiva, Synthesis of garnet structure compounds using aqueous sol-gel processing, 2004, Opt. Mater, vol. 26, pp.123-128.
20. H. Xian, X. Zhang, X. Li, H. Zou, M. Meng, Z. Zou, L. Gou, N. Tsubaki, Effect of the Calcination Conditions on the NO_x Storage Behavior of the Perovskite $BaFeO_{3-x}$ Catalysts, 2010, J. Catal. Today, vol. 158, pp. 215-219.
21. G.B. Jung, T.J. Huang, M.H. Huang, C.L. Chang, Preparation of samaria-doped ceria for solid-oxide fuel cell electrolyte by a modified sol-gel method, 2001, J. Mater. Sci vol. 36, pp. 5839-5844.